

Published in final edited form as:

Crit Care Med. 2009 January ; 37(1): 256–262. doi:10.1097/CCM.0b013e318192face.

Protective effects of nitric oxide synthase 3 and soluble guanylate cyclase on the outcome of cardiac arrest and cardiopulmonary resuscitation in mice

Takefumi Nishida, MD¹, Jia De Yu, BS¹, Shizuka Minamishima, MD¹, Patrick Y. Sips, PhD¹, Robert J. Searles, BS¹, Emmanuel S. Buys, PhD¹, Stefan Janssens, MD³, Peter Brouckaert, PhD⁴, Kenneth D. Bloch, MD^{1,2}, and Fumito Ichinose, MD¹

¹Anesthesia Center for Critical Care Research of the Department of Anesthesia and Critical Care, Massachusetts General Hospital and Harvard Medical School, Boston, MA

²Cardiovascular Research Center of the Department of Medicine at the Massachusetts General Hospital and Harvard Medical School, Boston, MA

³Centre for Transgene Technology and Gene Therapy, University of Leuven, Leuven, Belgium

⁴Department for Molecular Biomedical Research, Flanders Institute for Biotechnology (VIB) and Department of Molecular Biology, Ghent University, Ghent, Belgium

Abstract

Objectives—Despite advances in resuscitation methods, survival after out-of-hospital cardiac arrest remains very low, at least in part due to post cardiac arrest circulatory and neurological failure. To elucidate the role of nitric oxide (NO) in the recovery from cardiac arrest and CPR, we studied the impact of NOS3/cGMP signaling on cardiac and neurological outcomes after cardiac arrest and cardiopulmonary resuscitation (CPR).

Design—Prospective, randomized, controlled study

Setting—Animal research laboratory

Subjects—Mice

Interventions—Female wild-type mice (WT), NOS3-deficient mice (NOS3^{-/-}), NOS3^{-/-} mice with cardiomyocyte-specific overexpression of NOS3 (NOS3^{-/-}CSTg), and mice deficient for soluble guanylate cyclase α 1 (sGC α 1^{-/-}) were subjected to potassium-induced cardiac arrest (9 min) followed by CPR. Cardiac and neurological function and survival were assessed up to 24h post-CPR.

Measurements and Main Results—Cardiac arrest and CPR markedly depressed myocardial function in NOS3^{-/-} and sGC α 1^{-/-} but not in WT and NOS3^{-/-}CSTg. Neurological function score as well as 24h survival rate was lower in NOS3^{-/-} and sGC α 1^{-/-} compared to WT and NOS3^{-/-}CSTg. Detrimental effects of deficiency of NOS3 or sGC α 1 were associated with enhanced inflammation of heart and liver and increased cell death in heart, liver, and brain that were largely prevented by cardiomyocyte-restricted NOS3 overexpression.

Corresponding author: Fumito Ichinose, MD, Department of Anesthesia and Critical Care, Massachusetts General Hospital, 149 13th Street, 3405, Charlestown, Massachusetts 02129, Phone: 617-643-0987, Fax: 617-643-4490, fichinose@partners.org.

This is a PDF file of an unedited manuscript that has been accepted for publication. As a service to our customers we are providing this early version of the manuscript. The manuscript will undergo copyediting, typesetting, and review of the resulting proof before it is published in its final citable form. Please note that during the production process errors may be discovered which could affect the content, and all legal disclaimers that apply to the journal pertain.

Conclusions—These results demonstrate an important salutary impact of NOS3/sGC signaling on the outcome of cardiac arrest. Myocardial NOS3 prevented post-cardiac arrest myocardial dysfunction, attenuated end-organ damage, and improved neurological outcome and survival. Our observations suggest that enhancement of cardiac NOS3 and/or sGC activity may improve outcome after cardiac arrest and CPR.

Keywords

cardiac arrest; cardiopulmonary resuscitation; nitric oxide; neurological dysfunction; myocardial dysfunction; apoptosis

INTRODUCTION

It is estimated that approximately 500,000 people suffer cardiac arrest each year in the United States. Despite advances in resuscitation methods, including therapeutic hypothermia (1), cardiopulmonary resuscitation (CPR) is all too frequently unsuccessful. Although neurological injury appears to be the major cause of morbidity and death after cardiac arrest (2), post-cardiac arrest myocardial dysfunction also contributes significantly to mortality (3). However, molecular mechanisms responsible for myocardial dysfunction after cardiac arrest/CPR remain incompletely understood.

Nitric oxide (NO) is produced from NO synthases (NOS1, NOS2, and NOS3). One of the primary targets of NO is soluble guanylate cyclase (sGC). sGC is a heterodimer, composed of α_1 and β_1 subunits in the myocardium. NO binds to the heme moiety of sGC and stimulates the synthesis of the intracellular second messenger cGMP (4). NO attenuates ischemia-reperfusion (IR) injury in various organs including heart. For instance, overexpression of NOS3 in endothelial cells (5) or cardiomyocytes (6) attenuates IR injury in the heart, whereas NOS3 deficiency has been reported to exacerbate IR-induced myocardial stunning (7). While these observations support the protective role of NO/NOS3 in myocardial IR injury, the role of NO on the outcome of cardiac arrest remains incompletely defined, at least in part, due to the complex pathophysiological features of the post-cardiac arrest syndrome.

In the current study, we examined the impact of NOS3/cGMP-dependent signaling on myocardial and neurological function after cardiac arrest/CPR in mouse. We hypothesized that myocardial NOS3 confers protection against cardiac arrest/CPR-induced myocardial dysfunction via a cGMP-dependent manner. To address this hypothesis, we studied wild-type (WT), NOS3-deficient mice (NOS3^{-/-}), NOS3^{-/-} mice with cardiomyocyte-restricted overexpression of NOS3 (NOS3^{-/-}CSTg), and sGC α 1-deficient mice (sGC α 1^{-/-}). Here, we report that deficiency of NOS3 or sGC α 1 markedly worsens myocardial function and survival after cardiac arrest in mice.

MATERIALS AND METHODS

Mouse

After approval by the Massachusetts General Hospital Subcommittee on Research Animal Care, we studied 2- to 4-month-old female WT, NOS3^{-/-}, NOS3^{-/-} CSTg, and sGC α 1^{-/-} backcrossed 10 generations onto a C57BL/6 background. Female mice were used based on the model used in a previously published paper (8). NOS3^{-/-} CSTg and sGC α 1^{-/-} were generated as previously described (9-11).

Animal preparation

Mice were anesthetized with 80 µg/g of ketamine HCl and 12 µg/g xylazine HCl delivered by intraperitoneal injection and mechanically ventilated ($FiO_2=1.0$). Arterial blood pressure and left ventricular function were measured with a Millar conductance pressure-volume catheter (SPR-839, Millar Instruments Inc) inserted through the right carotid artery as previously described (10). A saline-filled microcatheter (PE-10, Becton Dickinson) was inserted into the left jugular vein for fluid administration. Blood pressure and needle-probe ECG monitoring data were recorded and analyzed with the use of a PC-based data acquisition system.

Murine CPR model

Cardiac arrest was induced by administration of 0.08 mg/g potassium chloride through the jugular catheter, and was confirmed by loss of arterial pressure and asystolic rhythm as previously described (8). After 9 minutes of cardiac arrest, chest compressions were delivered using a finger at a rate of 340~360 beats per minute. Hypothermia was induced with a cooling blanket to achieve a temperature of $28\pm 0.5^\circ\text{C}$ at the initiation of CPR and mice were allowed to rewarm thereafter without active warming. Body temperature gradually returned to $30\pm 0.5^\circ\text{C}$ at 60 min after CPR and there was no difference in body temperature between all genotypes throughout the duration of experiments. Return of spontaneous circulation (ROSC) was defined as sustained systolic arterial pressure >60 mm Hg (12). Cardiac function was examined during the first 60 min and 24h after CPR. For the measurements of cardiac function 24h after CPR, mice were anesthetized with intraperitoneal administration of fentanyl 250 µg/kg and ketamine 100 mg/kg. Hemodynamic data were analyzed using a software (PVAN version 3.6, Millar Instruments). Mice subjected to sham operation that were not subjected to cardiac arrest were used as controls.

Assessment of neurological function

Neurological function was assessed at 24h after cardiac arrest and CPR or sham surgery using previously reported neurological function scoring system with modification (8).

Histological evaluation

Twenty four hours after cardiac arrest and CPR or sham surgery, mice were euthanized and brain, heart, and liver were harvested, fixed in 4% formalin in PBS, and embedded in paraffin. Brain was cut with microtome in coronal planes, and 6 µm-thick sections including the CA1 and CA3 sectors of the hippocampus were used for analysis of caspase-3 activation. For histological evaluation of the heart and liver, 6 µm-thick sections of left ventricle at mid-ventricular level and left lobe, respectively, were used.

Quantification of leukocyte recruitment to the heart and liver after cardiac arrest and CPR was performed on paraffin sections stained with anti-CD45 monoclonal antibodies (purified rat anti-mouse CD45, BD Biosciences, San Jose, CA). The number of CD45+ cells was manually counted by an investigator blinded to the genotype or treatment in three serial sections per mouse ($n=3$ for sham-operated and $n=3-4$ for mice subjected to cardiac arrest and CPR for each genotype). The average number of leukocytes per square millimeter of tissue area was reported.

Cell death was detected in cardiac, hepatic, and brain paraffin sections using the terminal deoxynucleotidyltransferase-mediated dUTP nick-end labeling (TUNEL) technique (DeadEnd Fluorometric TUNEL System, Promega Corporation, Madison, WI), as previously described (13). Sections were also stained with 4',6-diamidino-2-phenylindole dihydrochloride (DAPI, Vectashield mounting medium with DAPI, Vector Laboratories,

Burlingame, CA) to quantify total number of cells in the area of interest. TUNEL positive cells were counted in the middle left ventricular section in a short axis and left lobe of the liver and reported as fraction of the total cell count in the same area. TUNEL-positive neurons were manually counted in the CA1 and CA3 sectors of the hippocampus, and number of TUNEL-positive cells per square millimeters of examined area was reported.

Activation of caspase-3 was assessed by immunohistochemistry in paraffin-embedded brain sections using anti-cleaved caspase-3 antibody (1:80, polyclonal rabbit anti-cleaved caspase-3 antibody, Cell Signaling) according to the protocol recommended by the manufacturer. Cleaved caspase-3-positive neurons were manually counted in the CA1 and CA3 sectors of the hippocampus, and number of cleaved caspase-3-positive neurons per square millimeters of examined area was reported.

Measurement of gene expression

Total RNA was extracted from LV tissue using TRIzol reagent (Invitrogen), and cDNA was synthesized using MMLV-RT (Invitrogen). intercellular cell adhesion molecule 1(ICAM1), interleukin-1 β (IL-1 β), interleukin-6 (IL-6), hemoxygenase-1 (HO-1), NOS2, and 18S ribosomal RNA transcript levels were measured by real-time PCR using a Realplex 2 system (Eppendorf, Inc.) and primers for ICAM-1 (5'-GTGATGCTCAGGTATCCATCCA-3', 5'-CACAGTTCTCAAAGCACAGCG-3'), IL-1 β (5'-GCAACTGTTCTGAACTCAACT-3', 5'-ATCTTTTGGGGTCCGTCAACT-3'), IL-6 (5'-TAGTCCTTCCTACCCCAATTTCC-3', 5'-TTGGTCCCTAGCCACTCCTTC-3'), HO-1 (5'-AAGCCGAGAATGCTGAGTTCA-3', 5'-GCCGTGTAGATATGGTACAAGGA-3'), NOS2 (5'-ACATCGACCCGTCCACAGTAT-3', 5'-CAGAGGGGTAGGCTTGTCTC-3'), and 18s rRNA (5'-CGGCTACCACATCCAAGGAA-3', 5'-GCTGGAATTACCGCGGCT-3'). Changes in the relative gene expression normalized to levels of 18S rRNA were determined using the relative C_T method.

Statistical Analysis

All data are expressed as mean \pm SEM. Data were analyzed using ANOVA for repeated measures or one or two-way ANOVA with a Holm-Sidak *post hoc* test. If, during the statistical analysis of our data, the parametric assumption was violated (*i.e.*, normality test failed), one or two-way ANOVA on ranks with a Holm-Sidak *post hoc* test was used. Difference in survival rate was analyzed by Gehan-Breslow test.

RESULTS

Myocardial NOS3 attenuates myocardial dysfunction after cardiac arrest and CPR

The rate of ROSC was similar and above 95 % in all genotypes. While the CPR time (in seconds) to ROSC tended to be longer in NOS3^{-/-} (161 \pm 14) and sGC α 1^{-/-} (163 \pm 10) than in WT (126 \pm 7) and NOS3^{-/-}CSTg (143 \pm 12), differences between groups were not statistically significant. Baseline cardiac function parameters were similar among the four genotypes (Table 1 and Figure 1). HR was depressed similarly in all genotypes before cardiac arrest possibly due to the effects of anesthesia but recovered to the normal levels within the first hour in all genotypes after CPR except for sGC α 1^{-/-} mice that continued to have lower HR (Figure 1). Parameters of cardiac systolic function including cardiac output (CO), LV ejection fraction (EF), and maximum rate of LV pressure rise (dP/dt_{max}) were markedly depressed in NOS3^{-/-} and sGC α 1^{-/-} compared to WT during the first hour after CPR. The relaxation time constant τ , a load-insensitive measure of diastolic function, was markedly prolonged in NOS3^{-/-} and sGC α 1^{-/-} compared to WT after cardiac arrest. Cardiomyocyte-restricted overexpression of NOS3 prevented the decrement of cardiac function after cardiac arrest in NOS3^{-/-} mice.

Depression of CO persisted in NOS3^{-/-} and sGCα1^{-/-} at 24h after CPR (Table 1). While dP/dt_{max} was reduced in WT, NOS3^{-/-}, and sGCα1^{-/-} 24h after CPR, the magnitude of decrements of dP/dt_{max} was more marked in sGCα1^{-/-} compared to other genotypes. Load-insensitive indices of LV systolic function including end-systolic elastance (Ees) and preload-recruitable stroke work (PRSW) were depressed in NOS3^{-/-} and sGCα1^{-/-} but not in WT 24h after CPR. LV diastolic function, assessed by the relaxation time constant τ, was markedly impaired in NOS3^{-/-} and sGCα1^{-/-} 24 h after cardiac arrest. Again, cardiomyocyte-restricted overexpression of NOS3 prevented the depression of LV function in NOS3^{-/-} mice 24h after cardiac arrest (Table 1).

Taken together, these results suggest that deficiency of NOS3 or sGCα1 markedly worsen functional recovery of myocardial function after cardiac arrest and CPR. Cardiomyocyte-restricted overexpression of NOS3 rescues myocardial function after cardiac arrest and CPR in NOS3^{-/-}.

NOS3-deficiency worsened neurological function 24h after cardiac arrest and CPR

Neurological function was recovered by 24h after CPR in NOS3^{-/-}CSTg (P=NS compared to sham, Table1). Surviving WT, NOS3^{-/-} and sGCα1^{-/-} showed impaired neurological function 24h after cardiac arrest compared to sham-operated mice of respective genotype (P<0.05 vs sham). While NOS3^{-/-} exhibited markedly impaired neurological function compared to WT and NOS3^{-/-}CSTg, sGCα1^{-/-} tended to have better neurological score than NOS3^{-/-} (P=0.058) 24h after cardiac arrest.

NOS3-deficiency increased neutrophil infiltration in heart and liver 24h after cardiac arrest

The number of CD45+ cells in the heart and liver did not differ between genotypes after sham surgery. Cardiac arrest and CPR increased the number of CD45+ cells in the heart of WT, NOS3^{-/-}, and sGCα1^{-/-}, but not in the hearts of NOS3^{-/-}CSTg (Figure 2). The magnitude of increase of the CD45+ cells in the heart was greater in NOS3^{-/-} and sGCα1^{-/-} compared to WT after CPR. In liver tissues, the number of CD45+ cells increased only in NOS3^{-/-} but not in other genotypes after CPR.

NOS3 deficiency aggravated induction of inflammatory cytokines in the heart after CPR

To further examine the mechanisms responsible for the myocardial dysfunction after CPR, we assessed gene expression of inflammatory cytokines in the heart tissue 24h after cardiac arrest. Cardiac arrest induced ICAM-1, IL-1β, and IL-6 in WT, NOS3^{-/-}, and sGCα1^{-/-} but not in NOS3^{-/-}CSTg in the heart (Figure 3). HO-1 was induced by CPR similarly in WT and NOS3^{-/-} but not in sGCα1^{-/-} or NOS3^{-/-}CSTg 24h after CPR. The magnitude of gene expression of ICAM-1 and IL-6 was greater in NOS3^{-/-} than in WT, whereas cardiac arrest did not induce IL-1β and IL-6 in NOS3^{-/-}CSTg. iNOS expression levels were not increased 24h after cardiac arrest in the heart. These observations suggest that NOS3 deficiency promoted cardiac arrest-induced inflammatory cytokine induction in the heart.

Impact of deficiency of NOS3 or sGCα1 on cell death after cardiac arrest

The number of TUNEL positive nuclei increased in the hearts of NOS3^{-/-} and sGCα1^{-/-} but not in those of WT or NOS3^{-/-}CSTg 24h after CPR (Figure 4). While cardiac arrest and CPR increased the number of TUNEL positive nuclei in the liver of all genotypes, the magnitude of increase was greater in NOS3^{-/-} than in other genotypes (Figure 4). In the CA1 and CA3 region of the hippocampus, the number of TUNEL positive nuclei after cardiac arrest was greater in NOS3^{-/-} than in WT (Figure 5). The number of CA1 and CA3 neurons that stained positive for activated caspase-3 after cardiac arrest was greater in NOS3^{-/-}, sGCα1^{-/-}, and NOS3^{-/-}CSTg than in WT. Cardiomyocyte-specific

overexpression of NOS3 attenuated cardiac arrest-induced cell death and activation of caspase 3 in the CA1 and CA3 regions of the hippocampus in NOS3^{-/-} (Figure 5).

NOS3-deficiency decreases survival rate after cardiac arrest

While 2 out of 23 WT died within 24h after CPR, all 15 NOS3^{-/-}CSTg survived for 24h after cardiac arrest and CPR (Figure 6). Survival rate at 24h after cardiac arrest was markedly worse in NOS3^{-/-} (9 out of 21 died) and sGCα1^{-/-} (6 out of 15 died) than in WT and NOS3^{-/-}CSTg.

DISCUSSION

The current study revealed that congenital NOS3 deficiency markedly worsens myocardial and neurological function and survival after cardiac arrest/CPR in mice. Deficiency of sGCα1 depressed cardiac function and decreased survival after CPR to the similar extent as did NOS3 deficiency. Deficiency of either NOS3 or sGCα1 was associated with marked inflammation and increased cell death in the heart after cardiac arrest. While CPR caused cell death in liver in all genotypes, the number of dead cells and accumulated leukocytes in the liver were greater in NOS3^{-/-} than in other genotypes. Similarly, the number of dead hippocampal neurons was greater in NOS3^{-/-} than in WT and NOS3^{-/-}CSTg after CPR. Of note, cardiomyocyte-restricted overexpression of NOS3 rescued NOS3^{-/-} mice from myocardial and neurological dysfunction and death after cardiac arrest. Taken together, these observations suggest that NOS3 prevents post-cardiac arrest myocardial dysfunction, at least in part via sGC-dependent mechanisms, and improves outcome of cardiac arrest/CPR.

The potential impact of NO/NOS on the outcome of cardiac arrest remains incompletely understood. We designed this study to characterize the impact of NOS3 on post-cardiac arrest myocardial function by taking advantage of mice with varying levels of myocardial NOS3 expression. NOS3 deficiency markedly decreased CO during the first hour and at 24h after CPR compared to WT. This reduction of CO was primarily due to worsened LV function at both time points. Notably, load-insensitive measures of LV systolic and diastolic function were more severely depressed in NOS3^{-/-} than in WT, suggesting that endogenous levels of NOS3-derived NO importantly contributes to the recovery of myocardial function after cardiac arrest. The protective role of NOS3 on post-cardiac arrest myocardial function is further supported by our observation that myocardial-restricted overexpression of NOS3 prevented cardiac arrest-induced myocardial dysfunction. Taken together, these observations support the hypothesis that NOS3 protects myocardial function after cardiac arrest.

To elucidate the mechanisms responsible for the protective effects of NOS3 on myocardial function, we examined leukocyte accumulation, cytokine induction, and cell death in the heart tissue 24h after CPR. Depressed cardiac function of NOS3^{-/-} mice was associated with increased leukocyte accumulation, augmented expression of ICAM-1 and IL-6, and increased cell death. Our observations are consistent with the findings of Larmann and colleagues who demonstrated an important role of ICAM-1 and neutrophil recruitment in the cardiac arrest-induced organ dysfunction (14). Of note, cardiomyocyte-restricted overexpression of NOS3 largely prevented cardiac arrest-induced leukocyte accumulation, inflammatory cytokine induction, and cell death in the heart. These observations support the protective role of NOS3 in cardiac ischemia-reperfusion injury induced by cardiac arrest and CPR.

NOS3 deficiency decreased survival at 24h after CPR in the present study. In addition to the depressed myocardial function, the decreased survival in NOS3^{-/-} mice after cardiac arrest was also associated with impaired neurological function, increased hepatic leukocyte

accumulation, and increased cell death in the brain and liver. NOS3 deficiency has been shown to increase leukocyte accumulation and exacerbate hepatic injury after IR (15). The increased cell death in the hippocampus in NOS3^{-/-} mice after cardiac arrest is consistent with the protective role of NOS3 against cerebral ischemia (16). The observation that NOS3 deficiency promoted the cardiac arrest-induced caspase 3 activation in the CA1 and CA3 regions suggests that hippocampal cell death was at least in part caused by apoptosis. It is of note that NOS3 is more concentrated in CA1 hippocampal pyramidal neurons than in any other brain areas (17). It is likely that worsened ischemic injury of multiple organs contributed to the decreased survival of NOS3^{-/-} mice after cardiac arrest and CPR.

Interestingly, cardiomyocyte-restricted overexpression of NOS3 in NOS3^{-/-} mice markedly improved neurological function and survival after cardiac arrest. These beneficial effects of excess NOS3 in the heart were associated with attenuated leukocyte infiltration in the liver and decreased cell death in the liver and brain. It is possible that the protection of cardiac function by overexpressed NOS3 in the heart preserved organ perfusion thereby limiting ischemic end organ damage and improving survival in NOS3^{-/-} after CPR. Alternatively, it is also conceivable that excess NO produced from cardiomyocytes overexpressing NOS3 is transported to remote tissues as an NO-adduct, where NO protected organ function by anti-inflammatory and anti-apoptotic effects (18).

To elucidate the down-stream mechanisms whereby NOS3 confers protection on myocardial function after cardiac arrest and CPR, we examined impact of sGC deficiency by studying mice deficient for sGC α 1. We found that sGC α 1^{-/-} tended to have worse myocardial systolic function (e.g., dP/dt_{max}, see Table 1 and Figure 1) in the first hour and 24h after CPR than did NOS3^{-/-}. The detrimental impact of sGC α 1-deficiency was associated with increased leukocyte accumulation and cell death in the heart and increased 24h mortality similar to the effects of NOS3 deficiency. While these observations suggest that protective effects of NOS3 on myocardial function and survival after cardiac arrest are at least in part mediated via sGC-dependent mechanisms, they also suggest that sources of NO other than NOS3 and/or non-NO dependent sGC activators (e.g., carbon monoxide) may also confer salutary impact on cardiac function after cardiac arrest.

On the other hand, neurological dysfunction tended to be less marked in sGC α 1^{-/-} than in NOS3^{-/-} mice. Compared to NOS3 deficiency, deficiency of sGC α 1 tended to cause less leukocyte infiltration in the liver and caspase-3 activation in hippocampal neurons after cardiac arrest. It is possible that sGC α 1-deficiency failed to abolish protective effects of NOS3 in these tissues since another sGC isoform (sGC α 2 β 1) is expressed or another sGC α subunit (α 2) exist in this knockout mouse. It has been reported that sGC α 1 is the predominant α subunit in most tissues including the heart, while sGC α 2 has much lower expression levels in most tissues, except in the brain where in α 1 and α 2 are expressed at similar levels (19). Alternatively, cGMP-independent NO-dependent mechanisms (i.e., protein S-nitrosylation or antioxidant effects(20)) may be more important for organ protection in the liver or brain than they are in the heart.

Volatile anesthetic has been shown to mimic cardioprotective effects of ischemic preconditioning. While impact of ketamine on cardiac IR injury remains controversial, it is possible that ketamine may have affected the results in the current study. Potential influence of anesthetic should be carefully considered when interpreting the data obtained from animal models of cardiac arrest.

In summary, the current study revealed important salutary impact of NOS3/sGC signaling in a murine model of cardiac arrest and CPR. Cardiac NOS3 prevented post-cardiac arrest myocardial dysfunction and improved neurological outcome and survival. Our results with

sGC α 1 deficient mice suggest that outcome of CPR may be worse in the situations where sGC is functionally impaired (i.e., oxidized) by increased oxidative stress. Further examination of the down-stream mechanisms of the protective effects of NOS3/sGC may allow identification of novel molecular targets in the prevention and treatment of organ dysfunction and death after cardiac arrest.

Acknowledgments

Authors thank Dr. Christophe Adrie for valuable comments and Drs. Misako Shigematsu and Masako Nakano for technical help.

Sources of funding: This work was supported by grants from UGENT-BOF-GOA and FWO-Vlaanderen to PB and National Institute of Health Grants HL70896 to KDB and HL71987 and GM79360 to FL.

References

1. The Hypothermia after Cardiac Arrest Study Group. Mild Therapeutic Hypothermia to Improve the Neurologic Outcome after Cardiac Arrest. *N Engl J Med* 2002;346:549–556. [PubMed: 11856793]
2. Laver S, Farrow C, Turner D, et al. Mode of death after admission to an intensive care unit following cardiac arrest. *Intensive Care Med* 2004;30:2126–2128. [PubMed: 15365608]
3. Herlitz J, Ekstrom L, Wennerblom B, et al. Hospital mortality after out-of-hospital cardiac arrest among patients found in ventricular fibrillation. *Resuscitation* 1995;29:11–21. [PubMed: 7784718]
4. Friebe A, Koelsing D. Regulation of Nitric Oxide-Sensitive Guanylyl Cyclase. *Circ Res* 2003;93:96–105. [PubMed: 12881475]
5. Jones SP, Greer JJM, Kakkar AK, et al. Endothelial nitric oxide synthase overexpression attenuates myocardial reperfusion injury. *AJP - Heart and Circulatory Physiology* 2004;286:H276–H282. [PubMed: 12969888]
6. Elrod JW, Greer JJ, Bryan NS, et al. Cardiomyocyte-specific overexpression of NO synthase-3 protects against myocardial ischemia-reperfusion injury. *Arterioscler Thromb Vasc Biol* 2006;26:1517–1523. [PubMed: 16645153]
7. Hannan RL, John MC, Kouretas PC, et al. Deletion of endothelial nitric oxide synthase exacerbates myocardial stunning in an isolated mouse heart model. *J Surg Res* 2000;93:127–132. [PubMed: 10945953]
8. Abella BS, Zhao D, Alvarado J, et al. Intra-arrest cooling improves outcomes in a murine cardiac arrest model. *Circulation* 2004;109:2786–2791. [PubMed: 15159295]
9. Janssens S, Pokreisz P, Schoonjans L, et al. Cardiomyocyte-specific overexpression of nitric oxide synthase 3 improves left ventricular performance and reduces compensatory hypertrophy after myocardial infarction. *Circ Res* 2004;94:1256–1262. [PubMed: 15044322]
10. Ichinose F, Buys ES, Neilan TG, et al. Cardiomyocyte-Specific Overexpression of Nitric Oxide Synthase 3 Prevents Myocardial Dysfunction in Murine Models of Septic Shock. *Circ Res* 2007;100:130–139. [PubMed: 17138944]
11. Buys ES, Sips P, Vermeersch P, et al. Gender-specific hypertension and responsiveness to nitric oxide in sGC α 1 knockout mice. *Cardiovasc Res* 2008;79:179–186. [PubMed: 18339647]
12. Idris AH, Becker LB, Ornato JP, et al. Utstein-Style Guidelines for Uniform Reporting of Laboratory CPR Research: A Statement for Healthcare Professionals From a Task Force of the American Heart Association, the American College of Emergency Physicians, the American College of Cardiology, the European Resuscitation Council, the Heart and Stroke Foundation of Canada, the Institute of Critical Care Medicine, the Safar Center for Resuscitation Research, and the Society for Academic Emergency Medicine. *Circulation* 1996;94:2324–2336. [PubMed: 8901707]
13. Neilan TG, Blake SL, Ichinose F, et al. Disruption of nitric oxide synthase 3 protects against the cardiac injury, dysfunction, and mortality induced by doxorubicin. *Circulation* 2007;116:506–514. [PubMed: 17638931]

14. Larmann J, Schmidt C, Gammelin H, et al. Intercellular adhesion molecule-1 inhibition attenuates neurologic and hepatic damage after resuscitation in mice. *Anesthesiology* 2005;103:1149–1155. [PubMed: 16306726]
15. Kawachi S, Hines IN, Laroux FS, et al. Nitric Oxide Synthase and Postischemic Liver Injury. *Biochemical and Biophysical Research Communications* 2000;276:851–854. [PubMed: 11027558]
16. Huang Z, Huang PL, Ma J, et al. Enlarged Infarcts in Endothelial Nitric Oxide Synthase Knockout Mice Are Attenuated by Nitro-l-Arginine. *J Cereb Blood Flow Metab* 1996;16:981–987. [PubMed: 8784243]
17. Dinerman JL, Dawson TM, Schell MJ, et al. Endothelial Nitric Oxide Synthase Localized to Hippocampal Pyramidal Cells: Implications for Synaptic Plasticity. *PNAS* 1994;91:4214–4218. [PubMed: 7514300]
18. Elrod JW, Calvert JW, Gundewar S, et al. Nitric oxide promotes distant organ protection: evidence for an endocrine role of nitric oxide. *Proc Natl Acad Sci USA* 2008;105:11430–11435. [PubMed: 18685092]
19. Mergia E, Russwurm M, Zoidl G, et al. Major occurrence of the new $\alpha 2\beta 1$ isoform of NO-sensitive guanylyl cyclase in brain. *Cellular Signalling* 2003;15:189–195. [PubMed: 12464390]
20. Cauwels A, Bultinck J, Brouckaert P. Dual role of endogenous nitric oxide in tumor necrosis factor shock: induced NO tempers oxidative stress. *Cell Mol Life Sci* 2005;62:1632–1640. [PubMed: 15990956]

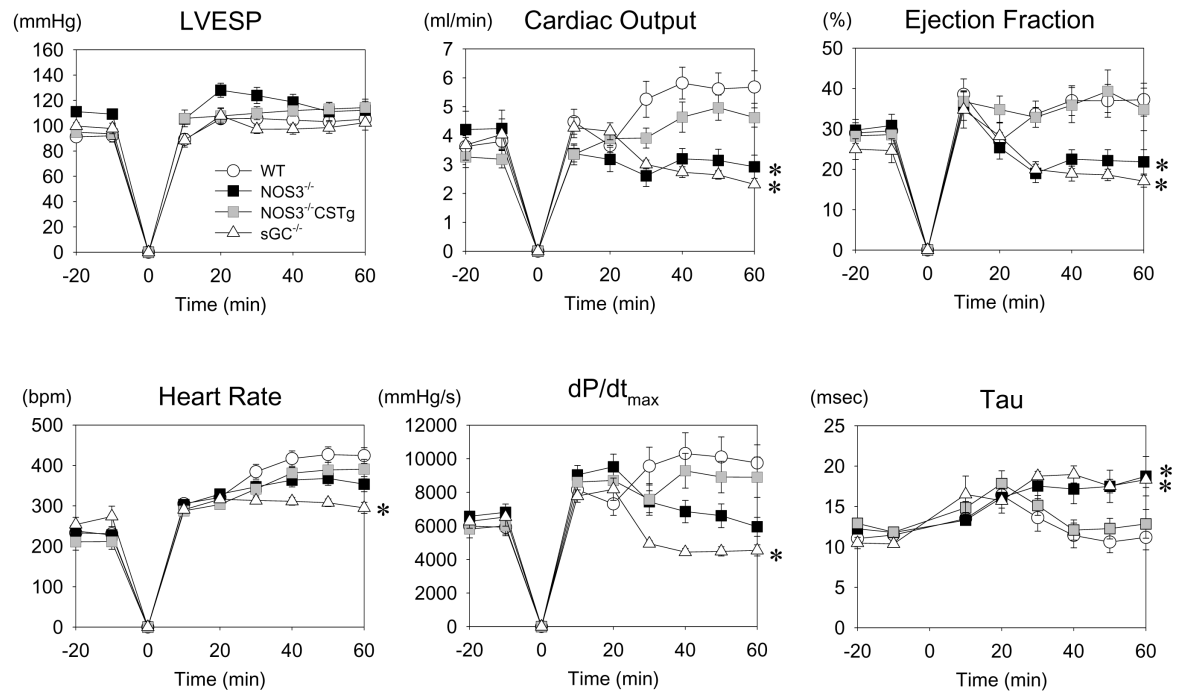


Figure 1.

Cardiovascular function before and during the first hour after cardiac arrest and cardiopulmonary resuscitation in WT (open circle), NOS3^{-/-} (black square), sGCα1^{-/-} (open triangle), and NOS3^{-/-}CSTg (gray square) mice. LVESP, left ventricular end-systolic pressure. dP/dt_{max}, maximum rate of left ventricular pressure rise. Tau, time constant of left ventricular isovolumic relaxation. *P<0.05 vs WT mice after CPR by repeated measures ANOVA.

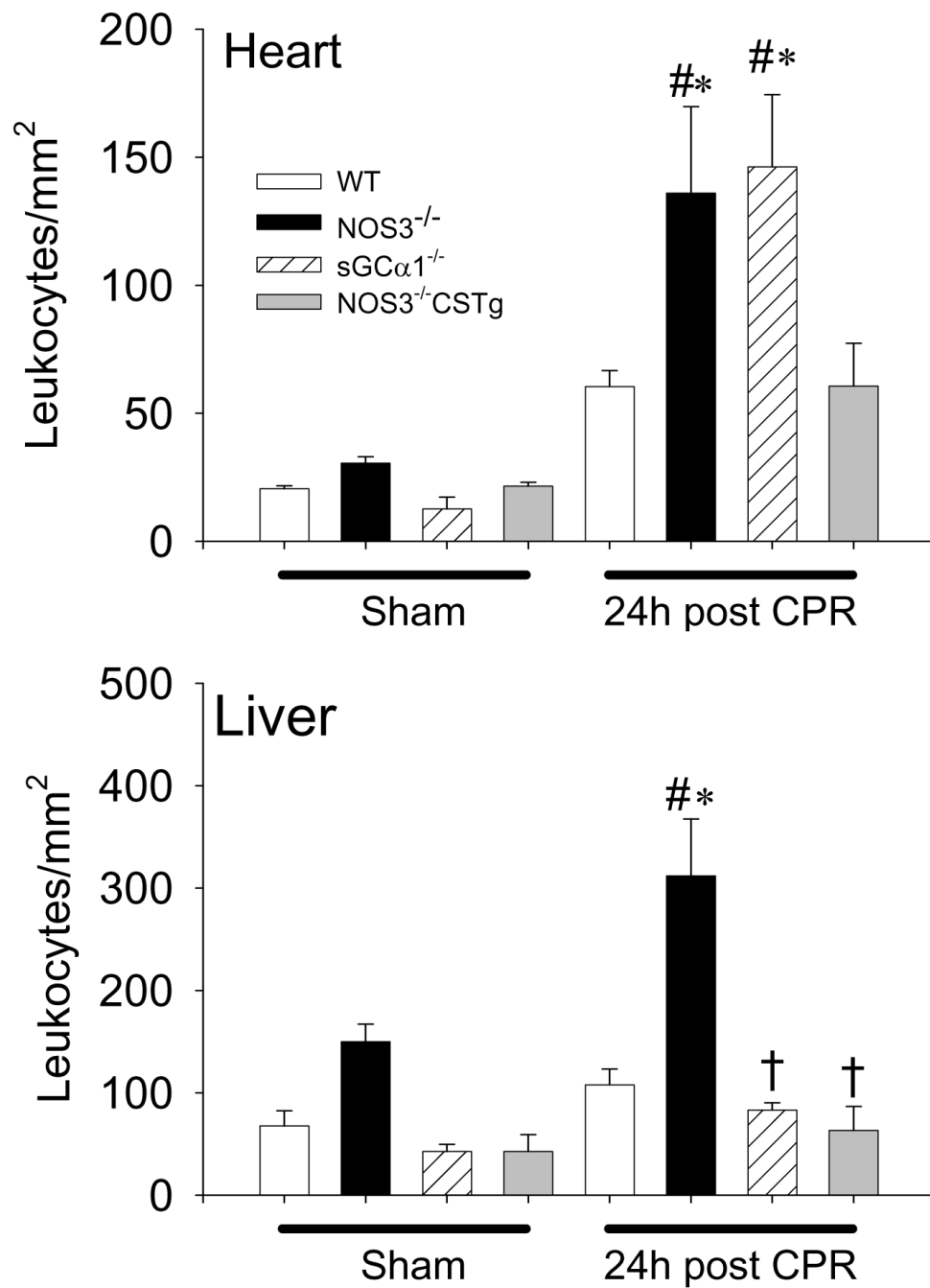


Figure 2. Number of CD45+ cells accumulating in the heart or liver 24h after sham operation or cardiac arrest and CPR in WT (open bar), NOS3^{-/-} (black bar), sGCα1^{-/-} (hatched bar), and NOS3^{-/-}CSTg (gray bar) mice. #P<0.05 vs sham-operated mice of the corresponding genotype. *P<0.05 vs WT after CPR. †P<0.05 vs NOS3^{-/-} after CPR (2-way ANOVA).

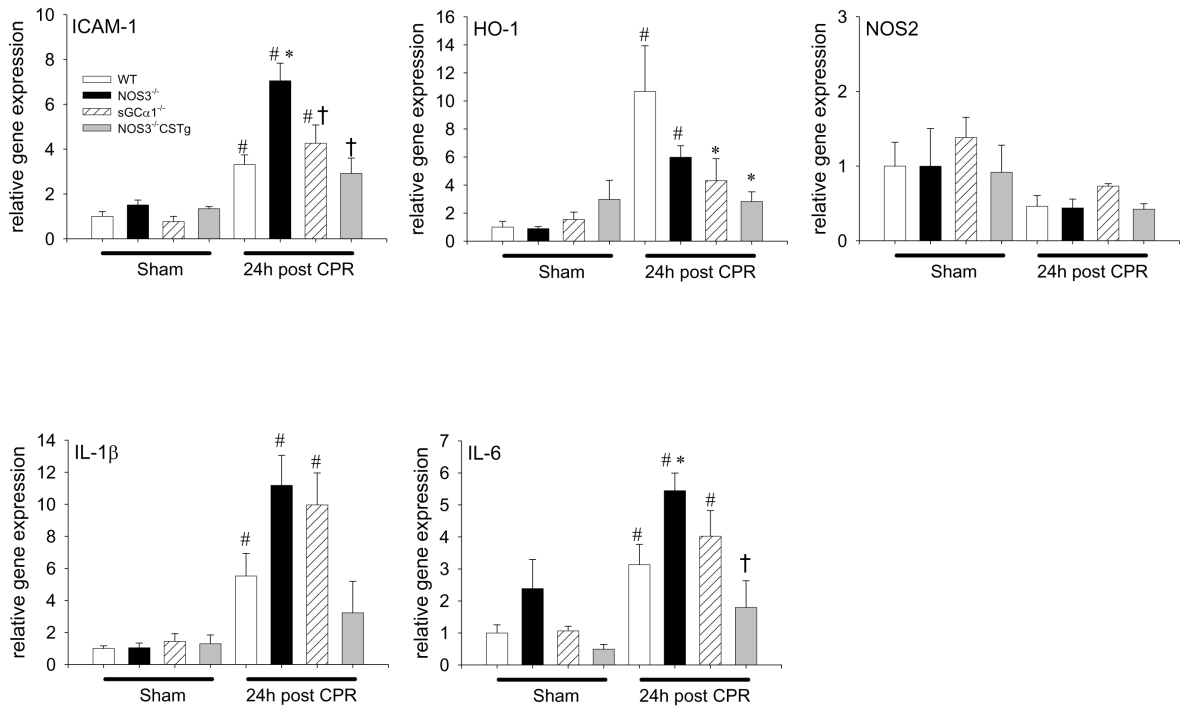


Figure 3.

Relative cardiac gene expression levels of ICAM-1, HO-1, IL-1 β , IL-6, and iNOS in the heart tissue of WT (open bar), NOS3^{-/-} (black bar), sGC α 1^{-/-} (hatched bar), and NOS3^{-/-}CSTg (gray bar) mice 24h after sham operation or cardiac arrest and CPR. #P<0.05 vs sham-operated mice of the corresponding genotype. *P<0.05 vs WT after CPR. †P<0.05 vs NOS3^{-/-} after CPR (2-way ANOVA).

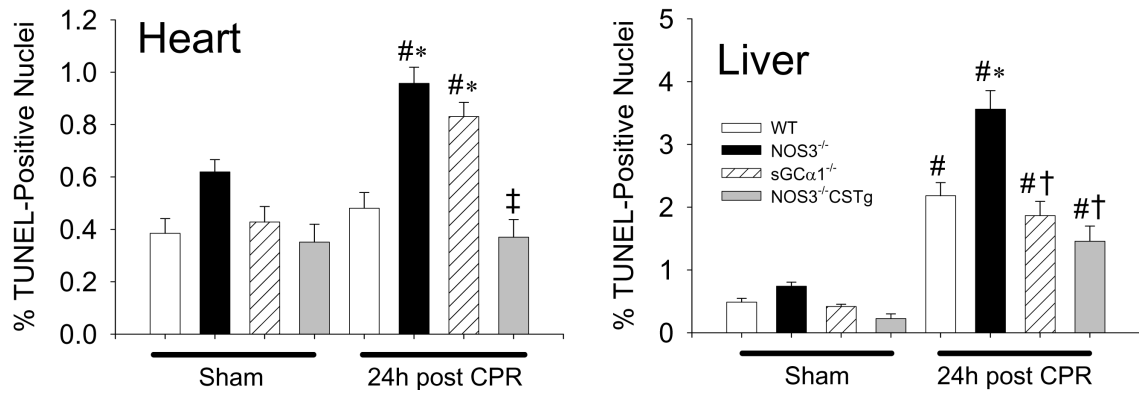


Figure 4.

Number of TUNEL-positive nuclei in the heart and liver 24h after sham operation or cardiac arrest in WT (open bar), NOS3^{-/-} (black bar), sGCα1^{-/-} (hatched bar), and NOS3^{-/-}CSTg (gray bar) mice. #P<0.05 vs sham-operated mice of the corresponding genotype. *P<0.05 vs WT after CPR. ‡P<0.05 vs NOS3^{-/-} and sGCα1^{-/-} after CPR. †P<0.05 vs NOS3^{-/-} after CPR (2-way ANOVA).

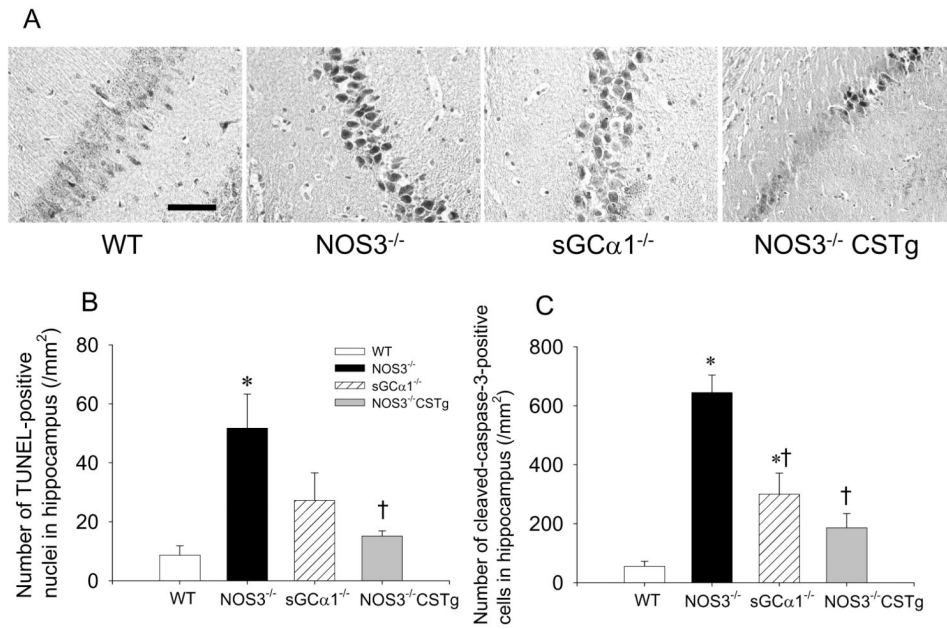


Figure 5. (A) Representative images of cleaved caspase-3 immunohistochemistry in the hippocampal CA1 region of WT, NOS3^{-/-}, sGCα1^{-/-}, and NOS3^{-/-} CSTg. Size bar indicates 50 μm. (B) Number of TUNEL-positive nuclei in the CA1 and CA3 regions of hippocampus in WT (open bar), NOS3^{-/-} (black bar), sGCα1^{-/-} (hatched bar), and NOS3^{-/-} CSTg (gray bar). (C) Number of the neurons stained positively with cleaved caspase-3 antibody in the CA1 and CA3 regions of hippocampus in WT (open bar), NOS3^{-/-} (black bar), sGCα1^{-/-} (hatched bar), and NOS3^{-/-} CSTg (gray bar). *P<0.05 vs WT after CPR. †P<0.05 vs NOS3^{-/-} after CPR (2-way ANOVA).

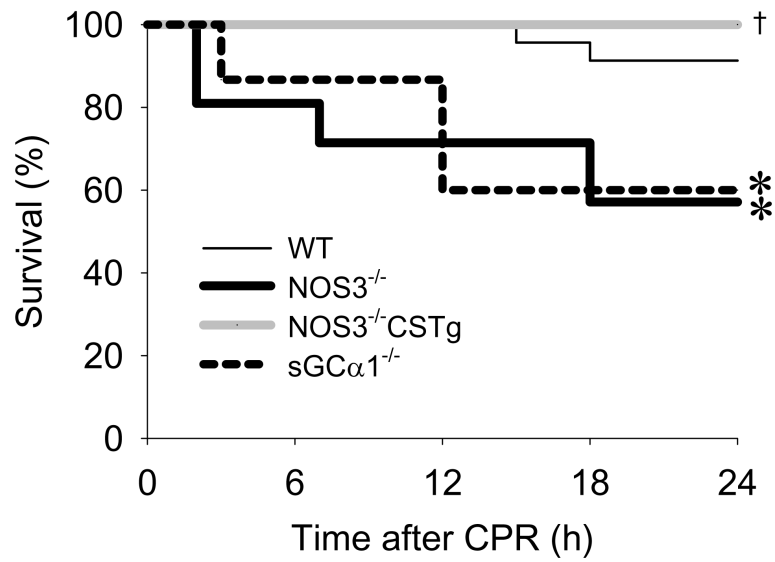


Figure 6. Survival after cardiac arrest and resuscitation in WT (thin solid line), NOS3^{-/-} (thick solid line), sGCα1^{-/-} (broken line), and NOS3^{-/-}CSTg (gray solid line) mice. Analysis of survival rate after cardiac arrest and CPR was performed with Gehan-Breslow method. *P<0.05 vs WT. †P<0.05 vs NOS3^{-/-} and sGCα1^{-/-}.

Table 1

Myocardial and neurological function 24 h after cardiac arrest and CPR

	WT			NOS3 ^{-/-}			sGCα1 ^{-/-}			NOS3 ^{-/-} CSTg		
	sham	CPR	n	sham	CPR	n	sham	CPR	n	sham	CPR	n
HR, bpm	583±36	584±21	5	538±44	546±22	5	596±28	517±25	5	608±23	566±20	5
LVEDP, mmHg	110±9	97±6	4±1	117±9	94±7*	3±0	114±9	78±8*†	2±1	123±9	109±6	3±1
LVEDP, mmHg	2±0	4±1	4±1	3±0	4±1	3±0	2±1	3±0	2±1	3±1	4±1	3±1
dP/dt _{max} , mmHg/s	19167±1655	14012±1234*	16909±1655	11814±1308*	8597±982	16209±1655	6304±1523*†	16273±1655	14060±1180	16273±1655	14060±1180	16273±1655
dP/dt _{min} , mmHg/s	-10421±927	-10870±927	-11363±965	-8597±982	-9920±570	-7534±1135	-10415±1966	-9398±879	-10415±1966	-9398±879	-9398±879	-9398±879
CO, ml/min	11.8±1.9	12.1±1.1	13.5±2.3	8.7±1.1*	11.5±1.6	6.3±1.3*#†	11.4±1.1	11.0±1.0	11.4±1.1	11.0±1.0	11.0±1.0	11.0±1.0
dP/dt _{max} /IP, s ⁻¹	222±8	208±9	201±15	174±15	202±19	158±18	210±21	200±14	210±21	200±14	200±14	200±14
Ees, mmHg/μL	32±7	23±5	28±7	8±6*	29±7	8±6*	24±7	28±5	24±7	28±5	28±5	28±5
PRSW, mmHg	199±4	140±14*	184±22	89±15*†	150±19	72±16*#†	142±30	158±14	142±30	158±14	158±14	158±14
τ, milliseconds	5.5±0.2	5.3±0.3	5.5±0.1	6.7±0.3*	5.5±0.4	6.3±0.4*	5.5±0.2	5.6±0.3	5.5±0.2	5.6±0.3	5.6±0.3	5.6±0.3
Neurological Function score	10±0	7±1*	10±0	4±1*#†	10±0	6±1*	10±0	9±1	10±0	9±1	9±1	9±1

Values are mean±SEM. Sham, sham-operated mice; HR, heart rate; LVEDP, left ventricular end-systolic pressure; LVEDP, left ventricular end-diastolic pressure; dP/dt_{max}, maximum rate of developed left ventricular pressure; dP/dt_{min}, minimum rate of developed left ventricular pressure; CO, cardiac output; dP/dt_{max}/IP, dP/dt_{max} divided by instantaneous pressure; Ees, left ventricular end-systolic elastance; PRSW, preload-recruitable stroke work; τ, time constant of isovolumic relaxation.

* P<0.05 vs sham-operated mice of the same genotype.

P<0.05 vs WT mice after cardiac arrest.

† P<0.05 vs NOS3^{-/-}CSTg after cardiac arrest.

‡ P<0.05 vs all other genotypes after cardiac arrest.